GNPNAT1 promotes the stemness of breast cancer and serves as a potential prognostic biomarker

HAO HU[1*], ZHI-WEN WANG[1*], SHUANG HU[2*], YUAN XIANG[3], YANG DENG[1], FU-JIAN WAN[1], TONG-CUN ZHANG[1], ZHONG-YI YANG[2] and XING-HUA LIAO[1]

[1]College of Life and Health Sciences, Institute of Biology and Medicine, Wuhan University of Science and Technology, Wuhan, Hubei 430000; [2]Yueyang People's Hospital, Yueyang Hospital Affiliated to Hunan Normal University, Yueyang Breast Disease Diagnosis and Treatment Technology Research Center, Yueyang, Hunan 414000; [3]Department of Medical Laboratory, Central Hospital of Wuhan, Tongji Medical College, Huazhong University of Science and Technology, Wuhan, Hubei 430000, P.R. China

Received March 7, 2023; Accepted May 26, 2023

DOI: 10.3892/or.2023.8594

Abstract. Glucosamine-phosphate N-acetyltransferase 1 (GNPNAT1) is a member of the acetyltransferase superfamily, related to general control non-depressible 5 (GCN5). It has been documented that GNPNAT1 expression is increased in lung cancer, whereas its involvement in breast cancer (BC) remains to be further investigated. The present study aimed to evaluate the expression levels of GNPNAT1 in BC and its effect on BC stem cells (BCSCs). The Cancer Genome Atlas (TCGA) database was used for the analysis of the expression of GNPNAT1 and its clinical significance. Cox regression and logistic regression analyses were used to evaluate prognosis-related factors. The GNPNAT1-binding protein network was constructed using the Search Tool for the Retrieval of Interacting Genes/Proteins (STRING) application. The biological signaling pathways implicated in GNPNAT1 were investigated through function enrichment analysis including Gene Ontology, Kyoto Encyclopedia of Genes and Genomes, and gene set enrichment analysis. The single-sample GSEA method was used to investigate the connection between the level of immune infiltration and GNPNAT1 expression in BC. GNPNAT1 expression was upregulated in patients with BC and was significantly associated with a poor prognosis. GNPNAT1 and its co-expressed genes were mostly enriched in nuclear transport, Golgi vesicle transport, ubiquitin-like protein transferase activity and ribonucleoprotein complex binding, as determined using functional enrichment analysis. GNPNAT1 expression was positively associated with Th2 cells and T-helper cells, and negatively associated with plasmacytoid dendritic cells, $CD8^+$ T-cells and cytotoxic cells. Additionally, the GNPNAT1 expression levels were considerably increased in BCSCs. GNPNAT1 knockdown markedly decreased the stemness ability of SKBR3 and Hs578T cells, including the production of CSC markers and mammosphere or clone formation, while GNPNAT1 overexpression increased the stemness level. Hence, the findings of the present study demonstrate that GNPNAT1 may be exploited as a novel prognostic biomarker and therapeutic target for BC.

Correspondence to: Professor Zhong-Yi Yang, Yueyang People's Hospital, Yueyang Hospital Affiliated to Hunan Normal University, Yueyang Breast Disease Diagnosis and Treatment Technology Research Center, 263 East Baling Road, Yueyanglou, Yueyang, Hunan 414000, P.R. China
E-mail: yangzhongyiyueyang@163.com

Professor Xing-Hua Liao, College of Life and Health Sciences, Institute of Biology and Medicine, Wuhan University of Science and Technology, 2 Huangjiahu West Road, Qingling Street, Hongshan, Wuhan, Hubei 430000, P.R. China
E-mail: xinghualiao@wust.edu.cn

*Contributed equally

Key words: glucosamine-phosphate N-acetyltransferase 1, prognosis, breast cancer, immune infiltration, breast cancer stem cells

Introduction

Breast cancer (BC) is amongst the most commonly encountered malignant tumors affecting women worldwide. According to the latest estimates from the International Agency for Research on Cancer of the World Health Organization, BC has superseded lung cancer as the most common type of cancer worldwide (1). Numerous changes and improvements have been made in the diagnosis and treatment of BC; however, a vast number of patients still presents with therapeutic resistance and relapse following surgery (2,3). Patients with BC continue to encounter significant clinical obstacles. Thus, it is crucial to improve the current diagnostic and treatment methods. Prognostic indicators for BC are critical for detection, diagnosis, prognosis and for the planning of therapeutic strategies (4). In spite of the discovery of several prognostic markers, the accuracy of BC prognosis remains limited, as indicated by the increased occurrence of BC tumors (5-7). Novel prognostic biomarkers with highly sensitive, specific and effective therapeutic targets

are necessary for the improvement of BC treatment and for the enhancement of patient clinical outcomes.

The gene for glucosamine-phosphate N-acetyltransferase 1 (GNPNAT1; also known as GNA1) is located at 14q22.1. This enzyme is crucial for the uridine diphosphate-N-acetylglucosamine biosynthetic pathway and nucleotide-sugar biosynthesis. Among the diseases related to GNPNAT1 are rhizomelic dysplasia and dysostosis multiplex, Ain-Naz type (8-10). GNPNAT1 expression has been linked to the development of castration-resistant prostate cancer via the phosphatidylinositol 3-kinase/protein kinase B signaling pathway (11). In addition, GNPNAT1 silencing has been reported to regulate insulin secretion in pancreatic β-cells (12). Moreover, the reduced expression of GNPNAT1 has been shown to inhibit tumor cell adhesion and infiltration in lung cancer A549 cells (13). Additionally, a number of recently published studies have demonstrated that GNPNAT1 may serve as a biomarker for lung cancer prognosis (14-17). However, it is uncertain whether GNPNAT1 may function as a biomarker for BC, and its biological function in BC has not yet been fully elucidated.

Cancer stem cells (CSCs) are a minute portion of the diverse tumor population. It is considered that their capacity to self-renew and differentiate constitutes the initial stage in the development of malignancies. A poor treatment response, tumor recurrence and metastasis in BC have been associated with CSCs (18,19). BC stem cells (BCSCs) have been widely identified, with their most common markers being $CD44^+$, $CD24^-$ and aldehyde dehydrogenase positive ($ALDH^+$) (20,21). There is increasing evidence to indicate that targeting CSCs may be an effective cancer therapy. However, further CSCs-related criteria and processes need to be identified.

In the present study, GNPNAT1 expression and prognosis of breast invasive carcinoma (BRCA) patients were analyzed using The Cancer Genome Atlas (TCGA) database. Additionally, the functional network of GNPNAT1 and its co-expressed genes in BRCA was examined, in order to determine their involvement in the immune response to malignancies. The expression of GNPNAT1 and its effects on the stemness capacity of BCSCs were also investigated. The objective of the present study was to identify novel biological targets and methods for the diagnosis, treatment, and prediction of the outcomes of patients with BC.

Materials and methods

Data collection and analysis. The toil program has been always used to acquire the RNA-sequencing data from UCSC Xena in TPM format (https://xenabrowser.net/datapages/). Genotype Tissue Expression Project (GTEx) and TCGA_BRCA normal tissue data were utilized to compare the two groups. From the TCGA and GTEx datasets, the mRNA expression profiles and clinical information of patients with BC were retrieved.

The University of Alabama at Birmingham Cancer data analysis portal (UALCAN) database analysis. UALCAN (http://ualcan.path.uab.edu/analysis.html) provides protein expression analysis options for 13 commonly occurring cancers, including BC, by using information from the Clinical Proteomic Tumor Analysis Consortium (CPTAC) dataset (22-25). Using the UALCAN database, data from GNPNAT1 protein expression analysis across BRCA and normal samples based on TCGA_BRCA data and the study of positively linked genes were obtained.

Human protein atlas (HPA) database analysis. The HPA database (https://proteinatlas.org/) provides information on protein levels in normal and cancer tissues for human gene expression profiling, focusing on various aspects of research on human proteins across the whole genome (26). Using HPA, the comparison between GNPNAT1 protein levels in normal vs. BC tissues was performed.

Gene Expression Profiling Interactive Analysis 2 (GEPIA2) database analysis. GEPIA2 (http://gepia2.cancer-pku.cn/#index) is an open access online database containing RNA sequencing expression data from 8,587 normal and 9,736 tumor samples (22). Various features of the 'Expression Analysis' module were used for visualization analysis, including analysis of tumor and normal differential expression, categorization by cancer type or pathological stage, assessment of patient survival, and detection of comparable genes. Pearson's correlation analysis was used to compute the correlation between GNPANT1 and other genes in BC.

LinkedOmics database analysis. LinkedOmics (http://www.linkedomics.org/login.php) is a powerful and free database site that includes multi-omics data from all 32 TCGA cancer types and 10 CPTAC cancer cohorts (27). The 'LinkFinder' module was used to analyze genes related with GNPNAT1 expression. Furthermore, the 'LinkInterpreter' module with the gene set enrichment analysis (GSEA) tool were used for Gene Ontology (GO) and Kyoto Encyclopedia of Genes and Genomes (KEGG) pathway enrichment analyses with the 'clusterProfile' R program.

WEB-based GEne SeT AnaLysis Toolkit (WebGestalt) database analysis. WebGestalt (http://www.webgestalt.org/), a web-based functional enrichment analysis software, was utilized to run a GSEA on GNPNAT1 for the present study (28). Using information from LinkedOmics, a WebGestalt dabatase was established with the following advanced parameters for GSEA: i) A category must include a minimum of 20 genes and a maximum of 500 genes; ii) the top 10 genes are relevant; and iii) 1,000 permutations are feasible.

Immune infiltration analysis. It is important to investigate and elucidate the links between tumor and immune cells in order to predict the immunotherapy response and develop novel immunotherapy targets. The TISIDB portal for tumor and immune system interactions (http://cis.hku.hk/TISIDB/index.php) incorporates several diverse data sources (29). Using database information, the amount and expression of GNPNAT1 in 28 tumor-infiltrating lymphocytes (TILs) were evaluated. Using gene expression profiling data from BC and the single-sample GSEA (ssGSEA) approach in the R package GSVA, the present study further examined the effect of GNPNAT1 expression on immune cell infiltration in depth (version 3.6). To analyze the association between the expression of GNPNAT1 and the number of immune cells that infiltrate tumors, the Wilcoxon rank sum test was used and Spearman's rank correlation coefficients were calculated.

Protein-protein interaction (PPI) networks. STRING (https://www.string-db.org/) is an online database for retrieval of interacting bases. In the present study, STRING was used to search for genes co-expressed with GNPNAT1 and to construct a PPI network.

Receiver operating characteristic (ROC) analysis. GNPNAT1 expression was compared between BRCA tumors and para-cancerous tissues by ROC analysis to test the predictive value of GNPNAT1 for BRCA diagnosis. The area under the ROC curve (AUC) is often used to evaluate diagnostic tests, and the AUC generally ranges from 0.5 to 1. The closer the AUC is to 1, the better the variable is in terms of predicting outcomes.

Establishment and evaluation of the nomogram. In the present study, GNPNAT1 expression and clinicopathologic characteristics of patients with BC, including age, T stage, N stage, M stage and TP53 form TCGA_BRCA database were used to create a nomogram, which is a reliable and useful method used to estimate a the overall survival (OS) of patients (30). The calibration curve was used to test and confirm that the nomogram was good at making predictions.

Cell culture. The MCF10A (cat. no. CL-0525) cell line was purchased from Wuhan Procell Company, derived from human normal mammary epithelial cells, and was cultured in specialized MCF10A medium (Procell Life Science & Technology Co., Ltd.). The human BC cell lines, SKBR3 (cat. no. 1101HUM-PUMC000085), MCF7 (cat. no. 1101HUM-PUMC000013) and Hs578T (cat. no. 1101HUM-PUMC000670), were cultured in DMEM (Dalian Meilun Biology Technology Co.) supplemented with 10% fetal bovine serum (Shanghai ExCell Biological Products Co., Ltd.), 100 U/ml penicillin and 100 μg/ml streptomycin (Dalian Meilun Biology Technology Co., Ltd.) in a 5% CO_2 incubator at 37˚C, while the MDA-MB-231 (cat. no. 1101HUM-PUMC000014) and MDA-MB-468 cells (cat. no. 1101HUM-PUMC000249) were cultured in RPMI-1640 medium (Dalian Meilun Biology Technology Co.). All the human BC cell lines were purchased from the ChineseNational Infrastructure of Cell line Resource (NICR).

Mammosphere formation assay. Briefly, serum-free DMEM/F12 medium (Dalian Meilun Biology Technology Co.) supplemented with epidermal growth factor (EGF; 20 ng/ml; T&L Biotechnology Co., Ltd), basic fibroblast growth factor (bFGF; 10 ng/ml; T&L Biotechnology Co., Ltd) and 2% B27 (Gibco; Thermo Fisher Scientific, Inc.) was used to enrich the SKBR3 and Hs578T CSCs in ultra-low adsorption six-well plates (Corning, Inc.) for 14 days at 37˚C in a 5% CO^2 incubator. Both the amount and the total number of CSCs were calculated.

Lentiviral transfection. The overexpression and knockdown vectors for GNPNAT1, LV-2 of a three-plasmid system including the GAG-POL and VSVG plasmid, were acquired from Tsingke Biotechnology Co., Ltd. The sh-GNPNAT1#1 sequence was 5'-GCAAGAAACTGAACTGTTACA-3'; the sh-GNPNAT1#2 sequence was 5'-GCTACGGCAACTCTGATTATA-3'; the sh-GNPNAT1#3 sequence was 5'-GGAGTTGTCAGC CCTGAACAA-3'. All plasmids (10 μg) were co-transfected into 293T cells (cat. no. 1101HUM-PUMC000091, NICR) with polyethylenimine (PEI) for lentivirus production. Use PEG8000 concentrated lentivirus solution (Beyotime Institute of Biotechnology) was used after 72 h. The SKBR3 and Hs578T cells were seeded, cultured to 60-70% confluency, and then transfected with lentivirus at a high concentration (MOI=10). Following a 72-h incubation, drug screening was initiated with 2 μg/ml puromycin and culture was continued for 2 weeks to establish a model of BC cells with stable overexpression or knockdown of GNPNAT1.

Reverse transcription-quantitative PCR (RT-qPCR). The RT-qPCR experiments were performed in accordance with a previously published study by the authors (31). Relative expression was calculated using Å (32). All reactions were performed in triplicate. The primer pair sequences used are presented in Table SI.

Western blot analysis. Protein extraction and western blot analysis were performed in accordance with the protocol stated in a previously published study by the authors (31). The primary antibodies used were as follows: GNPNAT1 rabbit mAb (1:2,000; cat. no. TD13048; Abmart Pharmaceutical Technology Co., Ltd.), Krüppel-like factor 4 rabbit mAb (KLF4; 1:2,000; cat. no. T56648; Abmart Pharmaceutical Technology Co., Ltd.), c-MYC rabbit mAb (1:2,000; cat. no. T55150; Abmart Pharmaceutical Technology Co., Ltd.), Nanog homeobox rabbit mAb (NANOG; 1:2,000; cat. no. T55611; Abmart Pharmaceutical Technology Co., Ltd.), and GAPDH rabbit mAb (1:2,000; cat. no. A19056; ABclonal Biotech Co., Ltd.). The secondary antibodies used here was HRP goat anti-rabbit IgG (H+L) antibody (1:2,000; cat. no. AS014; ABclonal Biotech Co., Ltd.)

Colony formation assay. Stably transfected BC cells overexpressing GNPNAT1 or cells in which GNPNAT1 was knocked down along with control cells were seeded into six-well plates and cultured for 14 days to obtain cell colonies. The colonies were fixed with 4% paraformaldehyde (Beyotime Institute of Biotechnology) for 20 min and then stained with 1% crystal violet solution (Beyotime Institute of Biotechnology) for 15 min at room temperature. The colonies were photographed using a mobile phone camera (Vivo) and counted.

Statistical analysis. GraphPad Prism 5.0 (Dotmatics) was used to conduct statistical analyses. At least three distinct experimental results were used for the acquisition of the mean and standard deviation. The unpaired Student's t-test was used to evaluate individual comparisons between two groups. Comparisons between three or more groups were determined using one-way ANOVA followed with Dunnett's post hoc test or Kruskal-Wallis test with Dunn's post hoc test. $P<0.05$ was considered to indicate a statistically significant difference.

Results

mRNA expression pan-cancer analysis of GNPNAT. Using the 'Gene DE' module of the TIMER2.0 database, the mRNA expression of GNPNAT1 in several types of tumors was investigated by comparing them to normal tissues adjacent to the tumors. As presented in Fig. 1A, GNPNAT1 expression

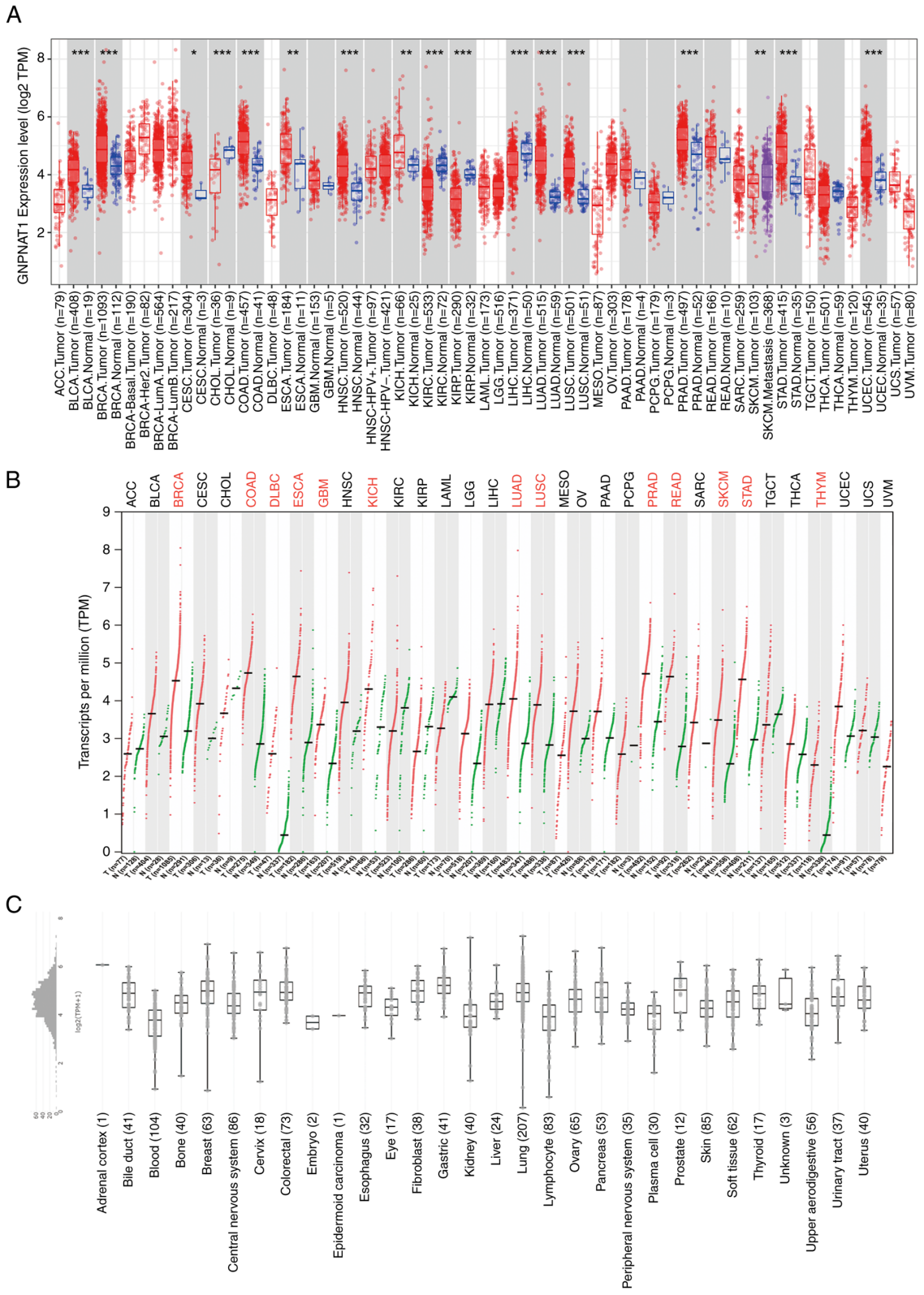

Figure 1. GNPNAT1 is significantly overexpressed in pan-cancer. (A) GNPNAT1 mRNA expression in different cancer types among TCGA in TIMER2.0. (B) GNPNAT1 mRNA expression in different cancer types among TCGA and GTEx in GEPIA2. (C) GNPNAT1 mRNA expression in human cancer cell lines, analyzing by the CCLE dataset. *P<0.05, **P<0.01 and ***P<0.001, as compared with the normal group. GNPNAT1, glucosamine-phosphate N-acetyltransferase 1; TCGS, The Cancer Genome Atlas; GTEx, Genotype Tissue Expression Project; GEPIA, Gene Expression Profiling Interactive Analysis 2; ACC, adenoid cystic carcinoma; BLCA, bladder urothelial carcinoma; BRCA, breast invasive carcinoma; CESC, cervical squamous cell carcinoma and endocervical adenocarcinoma; CHOL, cholangiocarcinoma; COAD, colon adenocarcinoma; DLBC, Diffuse large B cell lymphoma; ESCA, esophageal carcinoma; GBM, glioblastoma; HNSC, head and neck squamous cell carcinoma; KICH, kidney chromophobe; KIRC, kidney renal clear cell carcinoma; KIRP, kidney renal papillary carcinoma; LAML, acute myeloid leukemia; LGG, low-grade gliomas; LIHC, liver hepatocellular carcinoma; LUAD, lung adenocarcinoma; LUSC, lung squamous cell carcinoma; MESO, mesothelioma; OV, ovarian; PAAD, pancreatic adenocarcinoma; PCPG, pheochromocytoma and paraganglioma; PRAD, prostate adenocarcinoma; READ, rectum adenocarcinoma; SARC, sarcoma; SKCM, skin cutaneous melanoma; STAD, stomach adenocarcinoma; TGCT, tenosynovial giant cell tumor; THCA, thyroid carcinoma; THYM, thymoma; UCEC, uterine corpus endometrial carcinoma; UCS, uterine carcinosarcoma; UVM, uveal melanoma.

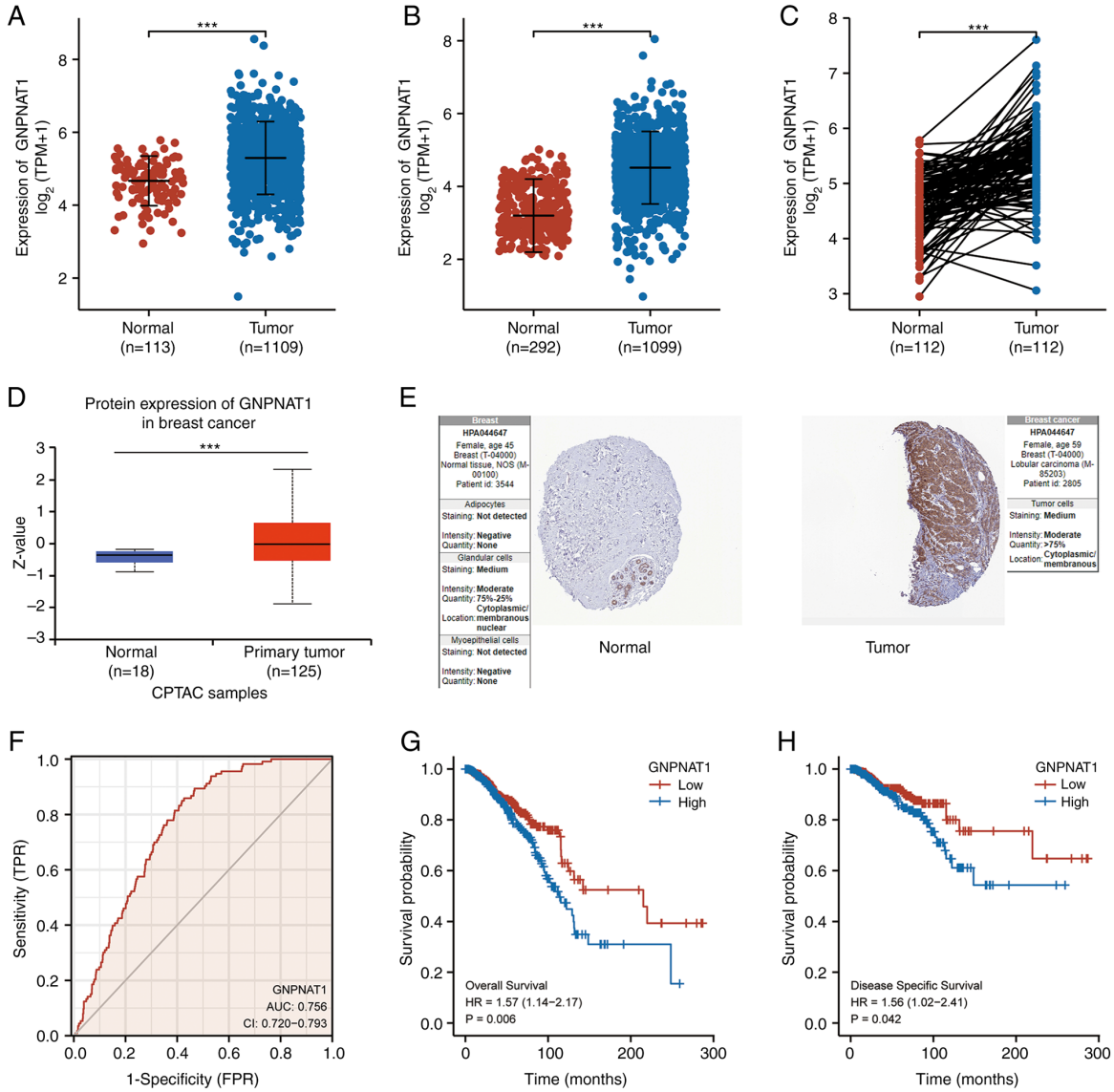

Figure 2. GNPNAT1 is highly expressed in BRCA. (A) GNPNAT1 mRNA expression comparison between unpaired normal and tumor tissues in TCGA_BRCA cohort. (B) GNPNAT1 mRNA expression comparison between unpaired normal and tumor tissues according to TCGA_BRCA and GTEx analyses. (C) GNPNAT1 mRNA expression comparison between paired normal and tumor tissues in the TCGA_BRCA cohort. (D) GNPNAT1 protein expression comparison between normal and tumor tissues obtained from the CPTAC dataset of the UALCAN database. (E) GNPNAT1 protein expression comparison between normal and tumor tissues obtained from the HPA database. (F) ROC curve was used to validate the prognostic value of GNPNAT1. (G) Kaplan-Meier analysis of the association between GNPNAT1 expression and OS in BRCA. (H) Kaplan-Meier analysis of the association between GNPNAT1 expression and DSS in BRCA. ***P<0.001. GNPNAT1, glucosamine-phosphate N-acetyltransferase 1; BRCA, breast invasive carcinoma; GTEx, Genotype Tissue Expression Project; CPTAC, Clinical Proteomic Tumor Analysis Consortium; UALCAN, The University of Alabama at Birmingham Cancer data analysis Portal; HPA, human protein atlas; DSS, disease-specific survival.

was overexpressed in bladder urothelial carcinoma (BLCA), BRCA, cervical squamous cell carcinoma and endocervical adenocarcinoma (CESC), colon adenocarcinoma (COAD), esophageal carcinoma (ESCA), head and neck squamous cell carcinoma (HNSC), lung adenocarcinoma (LUAD), lung squamous cell carcinoma (LUSC), kidney chromophobe (KICH), prostate adenocarcinoma (PRAD), stomach adenocarcinoma (STAD), uterine corpus endometrial carcinoma (UCEC) compared to normal tissues. However, cholangiocarcinoma (CHOL), kidney renal clear cell carcinoma (KIRC), liver hepatocellular carcinoma (LIHC), kidney renal papillary carcinoma (KIRP), and skin cutaneous melanoma (SKCM) presented with significantly reduced GNPNAT1 expression. The 'Expression Analysis-Profile Plots' tool on the GEPIA2 database was subsequently utilized to perform further research on the expression of GNPNAT1 in pan-cancer that matched TCGA normal and GTEx data. GNPNAT1 expression was significantly higher in BRCA, COAD, diffuse large B cell lymphoma (DLBCL), ESCA, glioblastoma (GBM), KICH, LUAD, LUSC, PRAD, rectum adenocarcinoma (READ), SKCM, STAD and thymic carcinoma (THYM) than in the control group (Fig. 1B). The 'CCLE Data Characterization Expression 22Q2 Public' module was used to assess GNPNAT1 mRNA expression in 30 cancer types, including 1,406 cell lines from the CCLE database. The findings demonstrated that the GNPNAT1 expression levels varied considerably across cancer cell lines (Fig. 1C).

Table I. Univariate and multivariate analyses of the association of GNPNAT1 expression with the overall survival of patients with breast cancer in TCGA_BRCA.

		Univariate analysis		Multivariate analysis	
Characteristic	Total no. of samples	Hazard ratio (95% CI)	P-value	Hazard ratio (95% CI)	P-value
Age, years	1,082				
≤60	601				
>60	481	2.020 (1.465-2.784)	<0.001	2.079 (1.437-3.008)	<0.001
T stage	1,079				
T1	276				
T2-T4	803	1.482 (1.007-2.182)	0.046	1.124 (0.599-2.106)	0.716
N stage	1,063				
N0	514				
N1-N3	549	2.239 (1.567-3.199)	<0.001	1.983 (1.266-3.107)	0.003
M stage	922				
M0	902				
M1	20	4.254 (2.468-7.334)	<0.001	2.915 (1.493-5.690)	0.002
Pathological stage	1,059				
Stage I	180				
Stage II-IV	879	2.210 (1.313-3.721)	0.003	1.257 (0.525-3.013)	0.608
GNPNAT1	1,082	1.213 (0.998-1.474)	0.052	1.082 (0.870-1.344)	0.479

GNPNAT1, glucosamine-phosphate N-acetyltransferase 1.

mRNA and protein expression analysis of GNPNAT1 in BC. The mRNA expression of GNPNAT1 was significantly increased in BC samples (n=1,109) in comparison with normal breast tissues (n=113) among TCGA (Fig. 2A). In contrast to the control group (n=292), GNPNAT1 expression remained substantially elevated in 1,099 BC samples with all of the normal samples when TCGA and the GTEx datasets merged (Fig. 2B). In addition, GNPNAT1 was highly expressed in 112 paired BC tissues (Fig. 2C). To further identify the protein expression of GNPNAT1, protein expression analysis using the CPTAC dataset provided by the UALCAN database was performed. The results revealed that primary breast tumors (n=125) presented with a significantly higher GNPNAT1 protein expression in comparison with the control group (n=18; P<0.001; Fig. 2D). In addition, GNPNAT1 protein was substantially expressed in tumor tissues in two representative immunohistochemistry images from the HPA collection (Fig. 2E).

Diagnostic and prognostic value analysis. ROC curve analysis was generated to evaluate the diagnostic value of GNPNAT1 for BRCA. The ROC curve indicated that the predictive ability of GNPNAT1 in BRCA had a relative accuracy with an area under the curve (AUC) of 0.756 [95% confidence interval (CI), 0.720-0.793], as presented in Fig. 2F. Kaplan-Meier (KM) survival curve analysis was used to evaluate and compare the survival differences between patients with a high and low expression of GNPNAT1 in TCGA_BRCA. The results revealed that a higher GNPNAT1 expression was associated with a poor OS and disease-specific survival (DSS). In detail, the median OS of the high GNPNAT1 expression group was 113.5 months, whereas in the low expression group it was 215.2 months (log-rank test; P=0.006; Fig. 2G). Similarly, the median disease specific survival of the high GNPNAT1 expression group was 122.3 months, and vs. 219.8 months in the low expression (log-rank test; P=0.042; Fig. 2H). Univariate and multivariate analyses of the association of the GNPNAT1 expression with OS among patients with BC was also performed in TCGA_BRCA. As demonstrated in Table I, in the univariate Cox analysis model, age (P<0.001), T stage (P=0.046), N stage (P<0.001), M stage (P<0.001) and pathological stage (P=0.003) were associated with OS in patients with BC; in the multivariate Cox analysis model, the associations of age (P<0.001), N stage (P=0.003) and M stage (P=0.002) with OS were preserved.

Analysis of patient clinicopathologic characteristics. To examine the association between GNPNAT1 mRNA expression and the clinicopathological characteristics of BC samples, logistic regression analysis and the Kruskal-Wallis test were used. Using age, T stage, M stage, N stage, pathological stage, prediction analysis of microarray 50 (PAM50), ER state, and ER status, GNPNAT1 mRNA expression was determined in TCGA_BRCA samples (Fig. 3). In all categories, the GNPNAT1 mRNA levels were increased in BRCA tumor tissues in comparison with normal tissues. The Wilcoxon rank sum test revealed an association between ethnicity (Caucasian) and GNPNAT1 mRNA expression (P<0.001; Table II). Using logistic regression, the connection between the level of GNPNAT1 expression and the clinicopathological characteristics of BC tissues was also investigated. The results revealed a significant association between GNPNAT1 expression and N

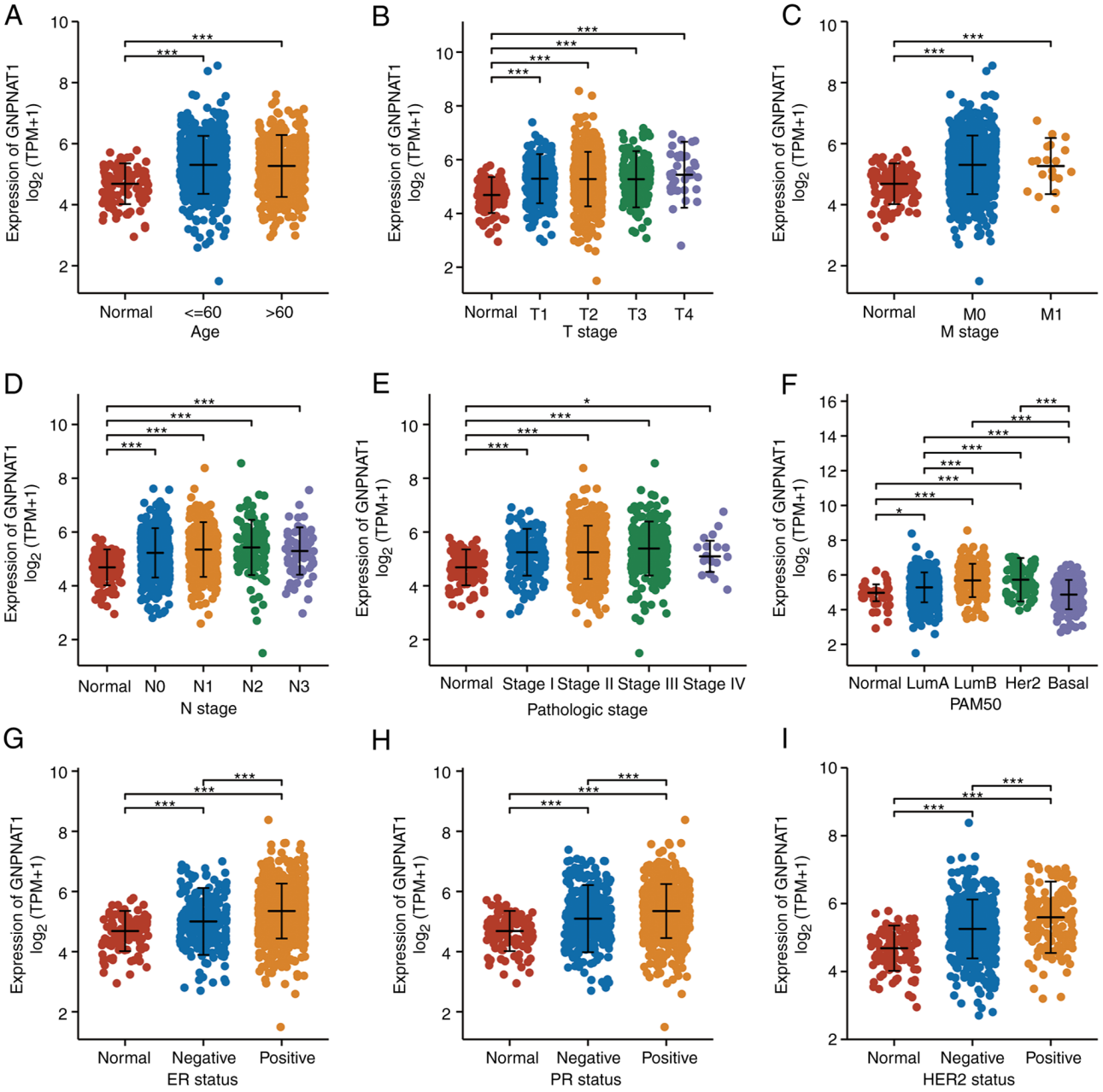

Figure 3. Association of GNPNAT1 expression with clinicopathological characteristics in TCGA_BRCA. Associations between GNPNAT1 mRNA expression and clinicopathological characteristics in BRCA patients based on (A) age, (B) T stage, (C) M stage, (D) N stage, (E) pathological stage, (F) PAM50, (G) ER status, (H) PR status and (I) HER2 status. *P<0.05 and ***P<0.001. GNPNAT1, glucosamine-phosphate N-acetyltransferase 1; PAM50, prediction analysis of microarray 50; ER, estrogen receptor; PR, progesterone.

stage (P=0.003), PR status (P<0.001), ER status (P<0.001) and HER2 status (P=0.001; Table III).

Co-expression gene analysis. Using LinkedOmics, GNPNAT1 co-expression networks in TCGA_BRCA cohort were obtained. The number of positively and negatively associated genes with GNPNAT1 was 6,137 and 7,494, respectively (FDR <0.01). As shown in Fig. 4A, dark red and green dots represent positively and negatively correlated genes, respectively. The top 50 most significantly co-expressed genes for both favorable and unfavorable outcomes were then utilized to generate heatmaps (Tables SII-III and Fig. 4B and C). Three genes were significantly positively linked with GNPNAT1 expression: The proteasome 26S subunit, ATPase 6 (PSMC6; Fig. 4D), L-2-hydroxyglutarate dehydrogenase (L2HGDH; Fig. 4E) and serine/threonine/tyrosine-interacting protein (STYX; Fig. 4F). Rho guanine nucleotide exchange factor 1 (ARHGEF1; Fig. 4G), the FES proto-oncogene, tyrosine kinase (FES; Fig. 4H) and AT-rich interaction domain 5A (ARID5A; Fig. 4I) were the three most significantly negatively correlated genes. Subsequently, a KM-OS curve analysis on the top 50 positively correlated genes was performed, using the survival analysis module of the GEPIA2 database. The results revealed that only three genes were highly expressed and associated with the poor prognosis in patient with BC, including tumor protein D52 (TPD52; Fig. 4J), signal recognition particle 54 (SRP54; Fig. 4K) and LRAT domain containing 2 (LRATD2, also known as FAM84B; Fig. 4L).

Table II. Association of GNPNAT1 expression with clinicopathological characteristics in breast cancer.

Characteristic	Low expression of GNPNAT1 (n=541)	High expression of GNPNAT1 (n=542)	P-value
Age, n (%)			0.411
≤60	293 (27.1%)	308 (28.4%)	
>60	248 (22.9%)	234 (21.6%)	
Race, n (%)			<0.001
Asian	23 (2.3%)	37 (3.7%)	
African American	119 (12%)	62 (6.2%)	
Caucasian	373 (37.5%)	380 (38.2%)	
T stage, n (%)			0.640
T1	137 (12.7%)	140 (13%)	
T2	318 (29.4%)	311 (28.8%)	
T3	72 (6.7%)	67 (6.2%)	
T4	14 (1.3%)	21 (1.9%)	
N stage, n (%)			0.013
N0	283 (26.6%)	231 (21.7%)	
N1	168 (15.8%)	190 (17.9%)	
N2	47 (4.4%)	69 (6.5%)	
N3	37 (3.5%)	39 (3.7%)	
M stage, n (%)			1.000
M0	438 (47.5%)	464 (50.3%)	
M1	10 (1.1%)	10 (1.1%)	
Pathological stage, n (%)			0.103
Stage I	98 (9.2%)	83 (7.8%)	
Stage II	323 (30.5%)	296 (27.9%)	
Stage III	106 (10%)	136 (12.8%)	
Stage IV	10 (0.9%)	8 (0.8%)	

GNPNAT1, glucosamine-phosphate N-acetyltransferase 1.

Table III. Associations of GNPNAT1 expression with clinicopathological features estimated by logistic regression analysis.

Characteristics	Total no. of samples	Odds ratio (OR)	P-value
Age (>60 vs. ≤60)	1,083	0.898 (0.706-1.141)	0.377
T stage (T2-T4 vs. T1)	1,080	0.966 (0.735-1.270)	0.807
N stage (N1-N3 vs. N0)	1,064	1.449 (1.138-1.846)	0.003
M stage (M1 vs. M0)	922	0.944 (0.384-2.322)	0.899
Pathologic stage (stage II-IV vs. Stage I)	1,060	1.183 (0.859-1.633)	0.304
PR status (positive vs. negative)	1,030	1.882 (1.447-2.454)	<0.001
ER status (positive vs. negative)	1,033	2.511 (1.858-3.416)	<0.001
HER2 status (positive vs. negative)	715	1.800 (1.257-2.596)	0.001
Radiation therapy (yes vs. no)	987	0.929 (0.722-1.194)	0.564

GNPNAT1, glucosamine-phosphate N-acetyltransferase 1; ER, estrogen receptor; PR, progesterone.

PPI network and functional enrichment analysis. The 'Similar Genes Detection' module was used to obtain 1,000 genes positively correlated with GNPNAT1 in the GEPIA2 database (Table SIV), and the 'Correlation' module was further used to obtain 1,608 genes positively correlated with GNPNAT1 in BRCA in the UALCAN database (Table SV). After using the Veen tool, the 'clusterProfile' R program was used to investigate GO and KEGG enrichment for 847 genes (Table SVI). As demonstrated in Fig. 5A, the majority of the genes were related to coated vesicles, the ubiquitin ligase complex, and cytoplasmic stress granules involved in nuclear transport, Golgi vesicle transport, ubiquitin-like protein

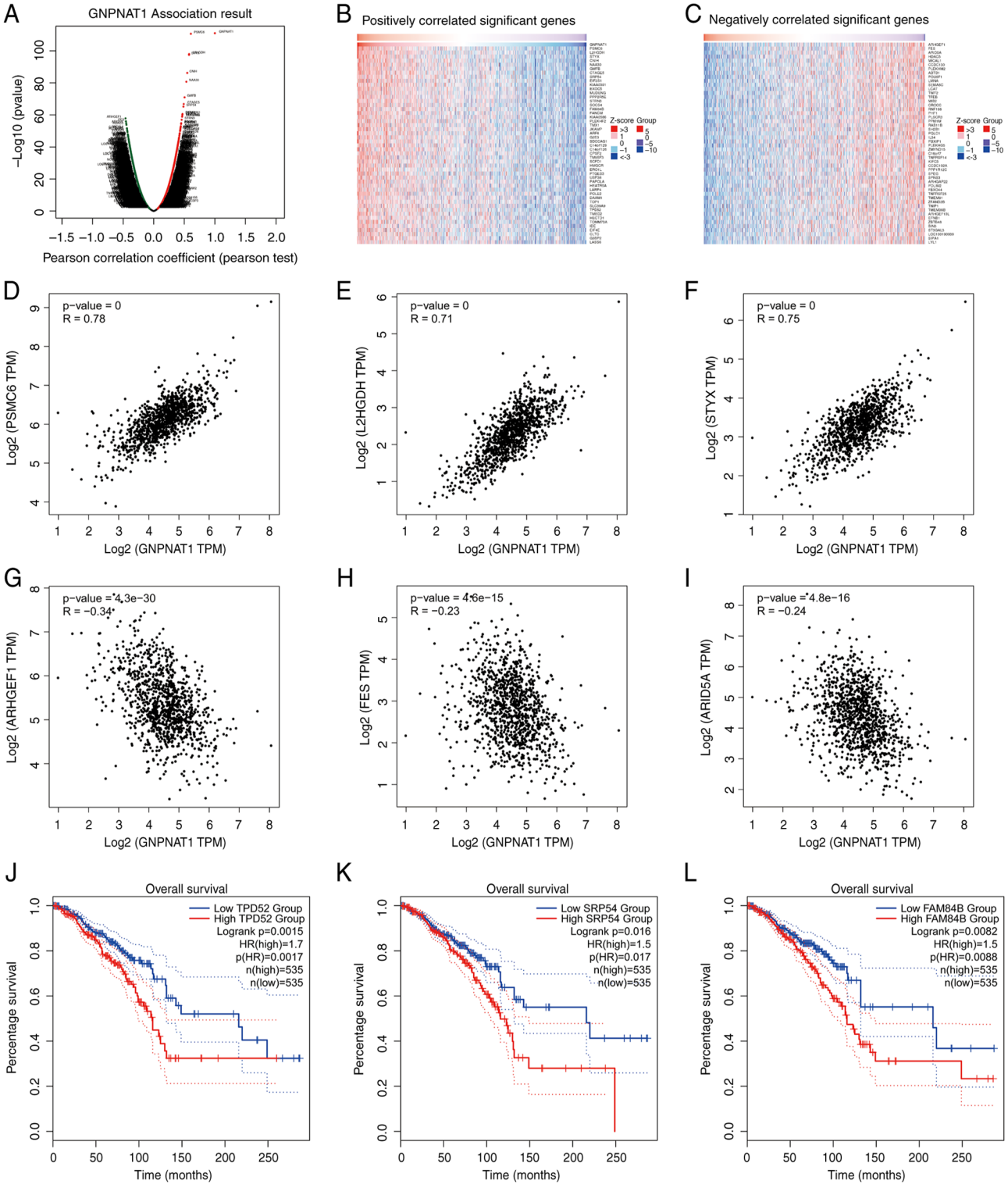

Figure 4. GNPNAT1 co-expression genes in TCGA_BRCA cohort. (A) The global GNPNAT1 highly correlated genes identified by Pearson's correlation analysis using RNAseq data on the HiSeq RNA platform in TCGA_BRCA cohort. Red and green dots represent positively and negatively significantly correlated genes with GNPNAT1, respectively. (B and C) Heatmaps showing top 50 genes positively and negatively correlated with GNPNAT1 in TCGA_BRCA. (D-F) Correlation analysis of GNPNAT1 between representative top three positively correlated genes: PSMC6, L2HGDH, STYX. (G-I) Correlation analysis of GNPNAT1 between representative top 3 negatively genes: ARHGEF1, FES, ARID5A. (J-L) OS curves of three positively correlated genes: TPD52, SRP54, FAM84B. GNPNAT1, glucosamine-phosphate N-acetyltransferase 1; PSMC6, the proteasome 26S subunit, ATPase 6; L2HGDH, L-2-hydroxyglutarate dehydrogenase; STYX, serine/threonine/tyrosine-interacting protein; ARHGEF1, Rho guanine nucleotide exchange factor 1; FES, FES proto-oncogene, tyrosine kinase; ARID5A, AT-rich interaction domain 5A; OS, overall survival; TPD52, tumor protein D52; SRP54, signal recognition particle 54; FAM84B, LRAT domain containing 2.

transferase activity, ribonucleoprotein complex binding, Salmonella infection and ubiquitin-mediated proteolysis, as revealed by the KEGG analysis results. For PPI network analysis, the interactions of 50 physically bound proteins with

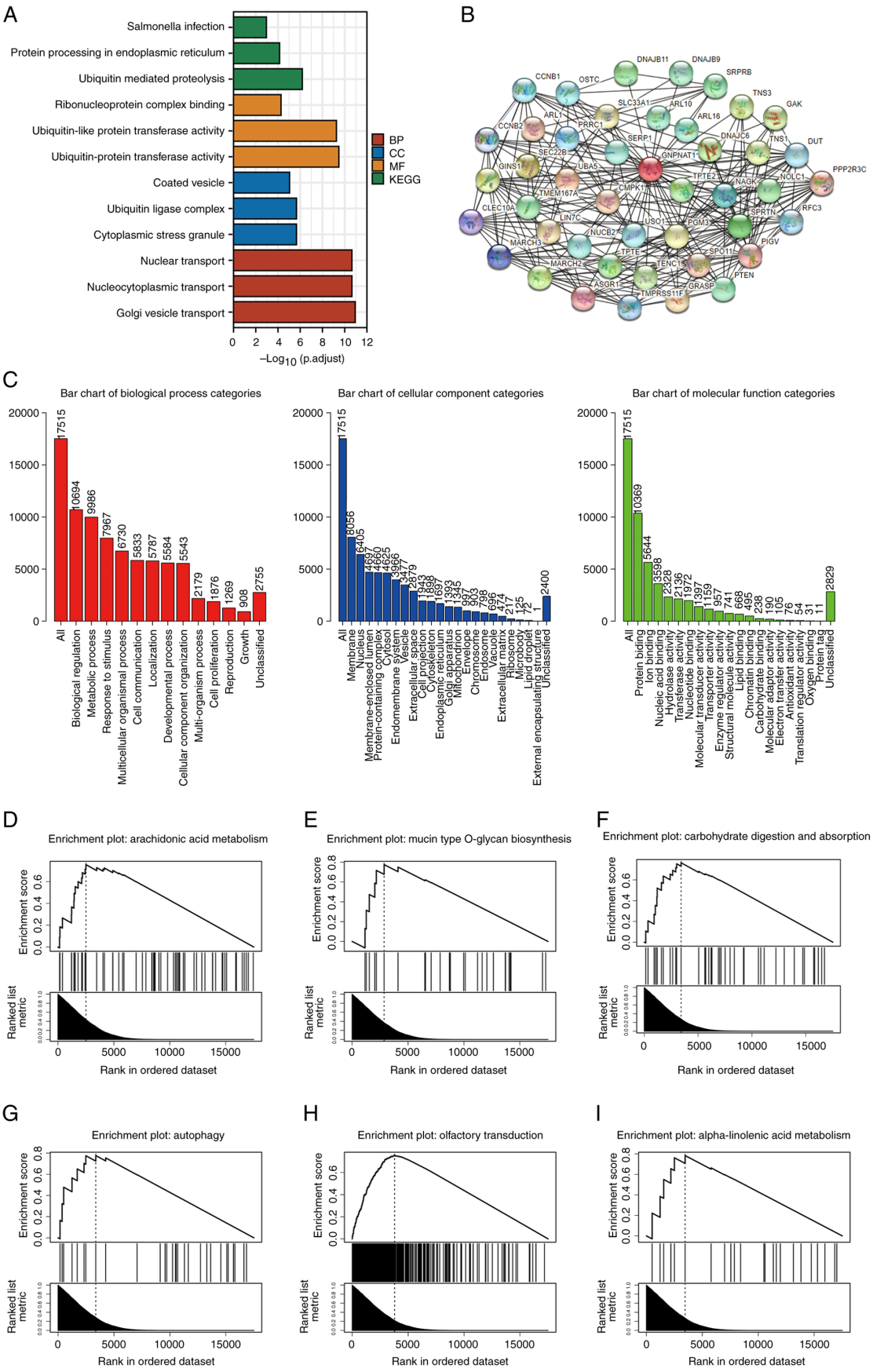

Figure 5. Functional enrichment analysis of GNPNAT1 in BC using GO, KEGG and GSEA. (A) A total number of 50 GNPNAT1-related proteins were identified using STRING. (B) GO terms (including BP, MF and CC) and KEGG of genes most strongly related with GNPNAT1. (C) GSEA analysis results of GNPNAT1 on GO terms. GSEA analysis results of GNPNAT1 on KEGG terms were: (D) Arachidonic acid metabolism, (E) Mucin type O-glycan biosynthesis, (F) Carbohydrate digestion and absorption, (G) Autophagy, (H) Olfactory transduction and (I) alpha-Linolenic acid metabolism. GNPNAT1, glucosamine-phosphate N-acetyltransferase 1; BC, breast cancer; GO, gene ontology; KEGG, Kyoto Encyclopedia of Genes and Genomes; GSEA, gene set enrichment analysis; BP, Biological Pathway; MF, Molecular Function; CC, Cellular Components.

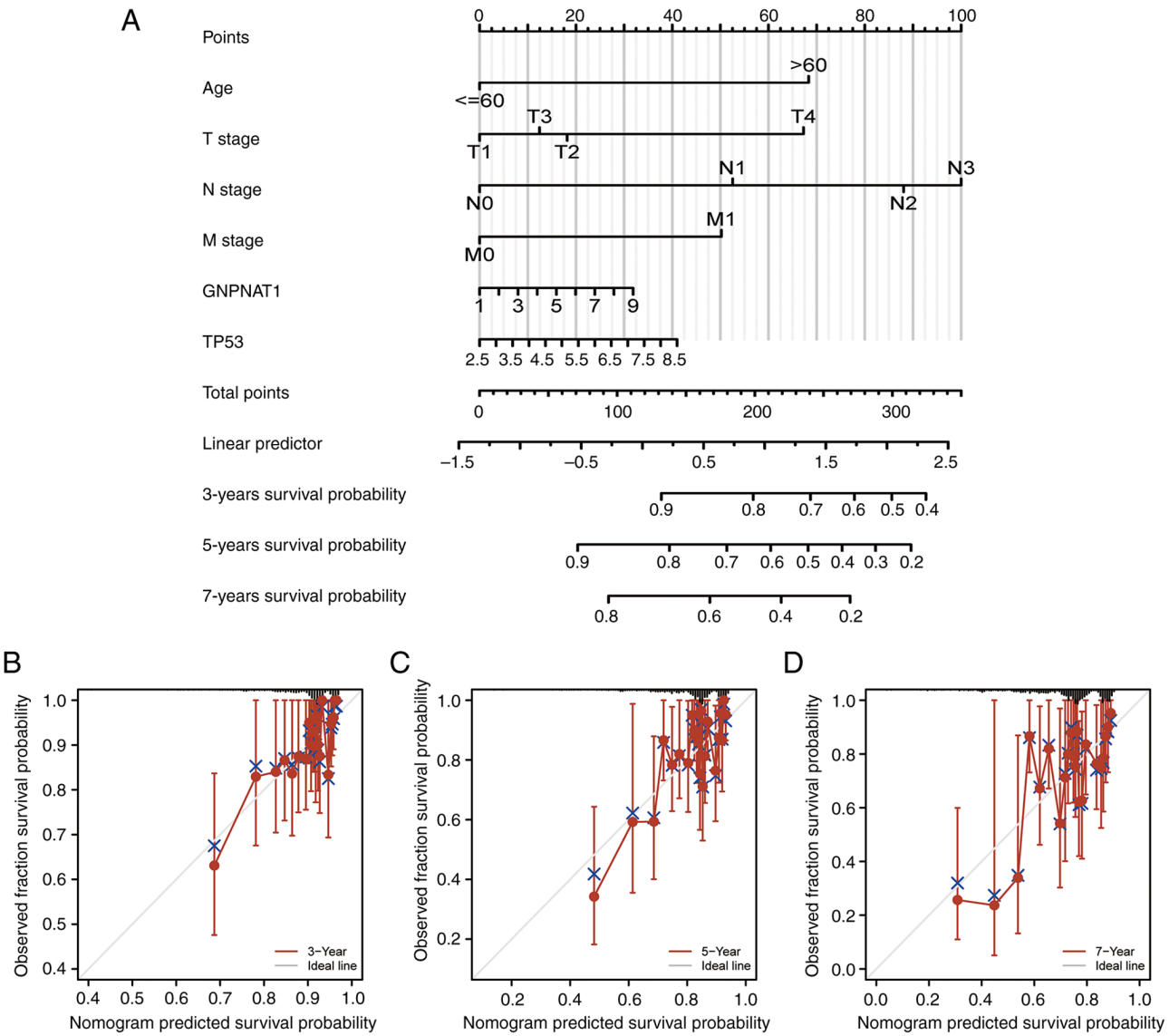

Figure 6. An OS nomogram with calibration curves for women diagnosed with BC. (A) A nomogram for estimating the likelihood of a patient surviving 3, 5, and 7 years after a BC diagnosis. (B) three-year, (C) five-year, and (D) seven-year OS rate calibration curves for a nomogram predicting these outcomes for BC patients. OS, overall survival; BC, breast cancer.

experimentally validated GNPNAT1-binding proteins were extracted from the STRING network (Fig. 5B).

For GSEA, data associated with GNPNAT1 (Table SVII) were upload on the WebGestalt database. The height of the bar, as revealed in Fig. 5C, indicates the total number of IDs in the user list category. For biological process categories, there were 10,694 genes associated with biological regulation; for cellular component categories, there were 8,056 genes associated with membrane; for molecular function categories, there were 10,369 genes associated with protein binding. The KEGG data analysis revealed the top six FDRs of pathways were arachidonic acid metabolism, mucin type O-glycan biosynthesis, carbohydrate digestion and absorption, autophagy, olfactory transduction and alpha-Linolenic acid metabolism (Fig. 5D-I).

Nomogram diagram and calibration analysis. The prognosis of patients with BC may now be predicted using a factor-based nomogram that is related to OS. As presented in Fig. 6A, prognosis worsens as the number of dots on the nomogram increases. In addition, a calibration curve was used to evaluate how predictions affected the nomogram (Fig. 6B-D). While using the bootstrapping technique, the nomogram's C-index was 0.702 (95% CI, 0.676-0.728), indicating a moderate degree of accuracy in predicting OS for patients with BC.

Immune infiltration analysis. According to the Spearman's Rho correlation analysis on the TISIDB database, the associations between the abundance of 28 TILs and expression of GNPNAT1 across human pan-cancer is presented in Fig. 7A. The red color indicates a positive correlation with GNPNAT1 mRNA expression, and blue indicates a negative correlation. In addition, the expression of GNPNAT1 was significantly positively correlated with the levels of immune cell infiltration of Th2 cells and T-helper cells and negatively correlated with plasmacytoid dendritic cells (pDCs), $CD8^+$ T-cells and cytotoxic T-cells (Fig. 7B). Furthermore, the enrichment scores of Th2 cells and T-helper cells in the GNPNAT1 high expression group were markedly higher than those in the GNPNAT1 low

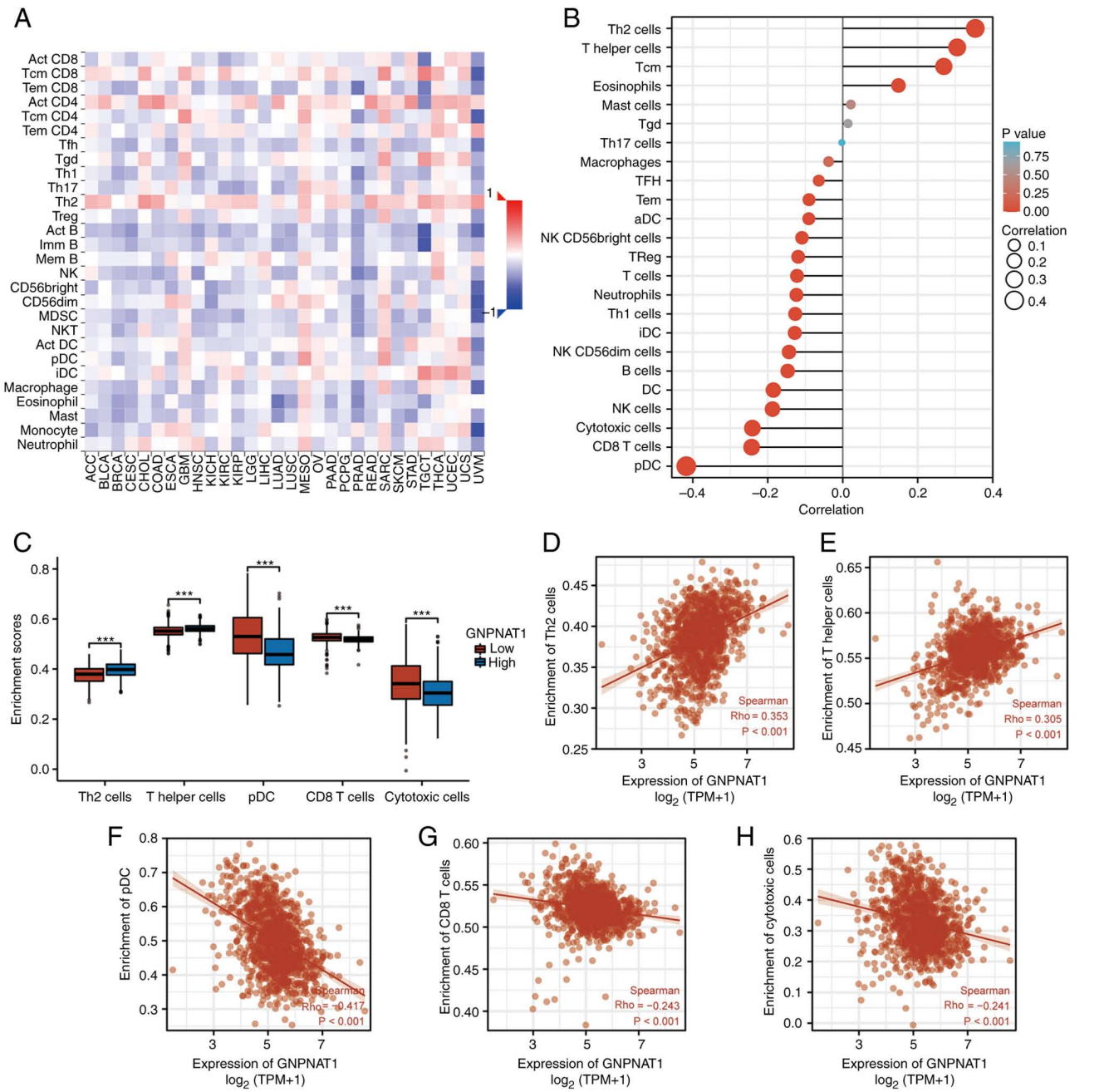

Figure 7. Correlation of GNPNAT1 expression with immune infiltration level in BC. (A) Correlation between GNPNAT1 expression and relative abundance of 28 types of TILs across human pan-cancer on TISIDB database. (B) Correlation between GNPNAT1 expression and relative abundance of 24 types of immune cell in BC. (C) Comparison of immune infiltration levels of immune cells (including Th2 cells, T-helper cells, pDC, $CD8^+$ T-cells and cytotoxic cells) between the high- and low-GNPNAT1 expression groups. (D-H) Correlations between the relative enrichment scores of immune cells (including Th2 cells, T-helper cells, pDC, $CD8^+$ T-cells and cytotoxic cells) and the expression of GNPNAT1. ***P<0.001. GNPNAT1, glucosamine-phosphate N-acetyltransferase 1; BC, breast cancer; TILs, tumour-infiltrating lymphocytes; pDC, plasmacytoid dendritic cells.

expression group, whereas the enrichment scores of pDC, CD8 T-cells and cytotoxic T-cells in the GNPNAT1 high expression group were markedly reduced, as compared with the GNPNAT1 low expression group (P<0.001 in all comparisons; Fig. 7C-H).

mRNA and protein expression analysis of GNPNAT1 in BC cells and CSCs. The Expression of GNPNAT1 was upregulated in the MCF7, SKBR3, Hs578T and MDA-MB-468 BC cell lines in comparison with the MCF10A normal breast cell line. Using RT-qPCR and western blot analysis, the mRNA (Fig. 8A) and protein (Fig. 8B) expression levels of GNPNAT1 were evaluated. GNPNAT1 expression in the SKBR3 and Hs578T cell lines was markedly higher than in the other cell lines. Thus, these two cell lines were used in further analyses. Moreover, GNPNAT1 expression was considerably increased in mammospheres, in relation to adherent cells (Fig. 8C and D). To determine whether BCSCs had been effectively enriched, the expression levels of CSC markers, including c-MYC, KLF4 and NANOG, were measured in mammosphere cells (Fig. 8E and F). The considerable increase in the mRNA and protein expression of CSC markers in breast spheroid cells revealed that the mammospheres included a high number of CSCs.

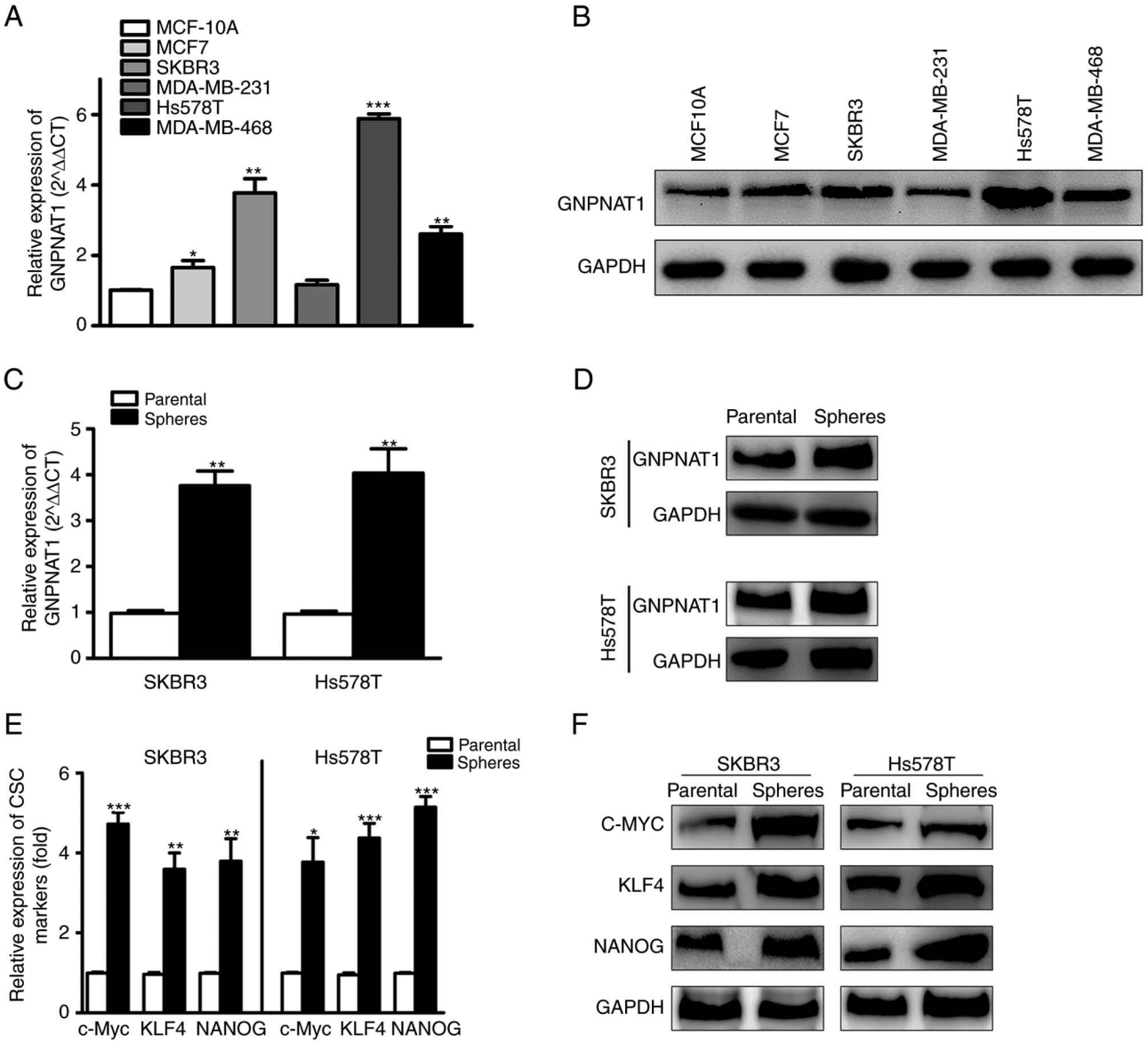

Figure 8. GNPNAT1 expression levels in BC. (A and B) GNPNAT1 mRNA and protein levels in BC cell lines. (C and D) mRNA and protein levels of GNPNAT1 in tumor-attached BC cells and mammospheres. (E and F) The mRNA and protein concentrations of CSC markers in tumor-attached BC cells and mammospheres. *P<0.05, **P<0.01, and ***P<0.001 vs. control. GNPNAT1, glucosamine-phosphate N-acetyltransferase 1; BC, breast cancer; CSC, cancer stem cells.

GNPNAT1 knockdown suppresses the stemness of BC cells. In order to determine whether GNPNAT1 participates in the control of BCSCs, GNPNAT1 was initially knocked down in the SKBR3 and Hs578T cell lines. As presented in Fig. 9A in three independent shRNA vector knockdown cell lines, shGNPNAT1#3 was the optimally functioning and was therefore used in subsequent experiments. Pluripotent transcription factors (c-MYC, KLF4 and NANOG) are frequently used to identify CSCs in clinical tissues and several cancer cell lines (33,34). The mRNA (Fig. 9B) and protein (Fig. 9C) levels of c-MYC, KLF4 and NANOG were examined using RT-qPCR and western blot analysis. Compared to the control cells, transfection with shGNPNAT1 resulted in a reduction in the mRNA and protein expression levels of stemness-related genes and GNPNAT1. Following GNPNAT1 knockdown, the capacity of SKBR3 and Hs578T cells to produce clones was drastically limited, according to colony formation test data (Fig. 9D and E). Moreover, the capacity of GNPNAT1 knockdown BC cells to produce tumor spheroids was evaluated. As demonstrated in Fig. 9F, GNPNAT1 knockdown resulted in fewer spheroids developing in the cells than in the vector control, as predicted. According to statistical examination of the number and diameter of spheroids, the number and size of the GNPNAT1 knockdown group decreased significantly (Fig. 9G and H). Therefore, it can be concluded that GNPNAT1 knockdown inhibited the stemness of BC cells.

GNPNAT1 overexpression promotes the stemness of BC cells. A cell line with the stable overexpression of GNPNAT1 was also constructed to examine its effect on the stemness capacity of BCSCs. As demonstrated in Fig. 10A, the GNPNAT1 mRNA levels were considerably elevated in the SKBR3 and Hs578T cell lines following transfection with a lentiviral GNPNAT1 overexpression vector. The mRNA (Fig. 10B)

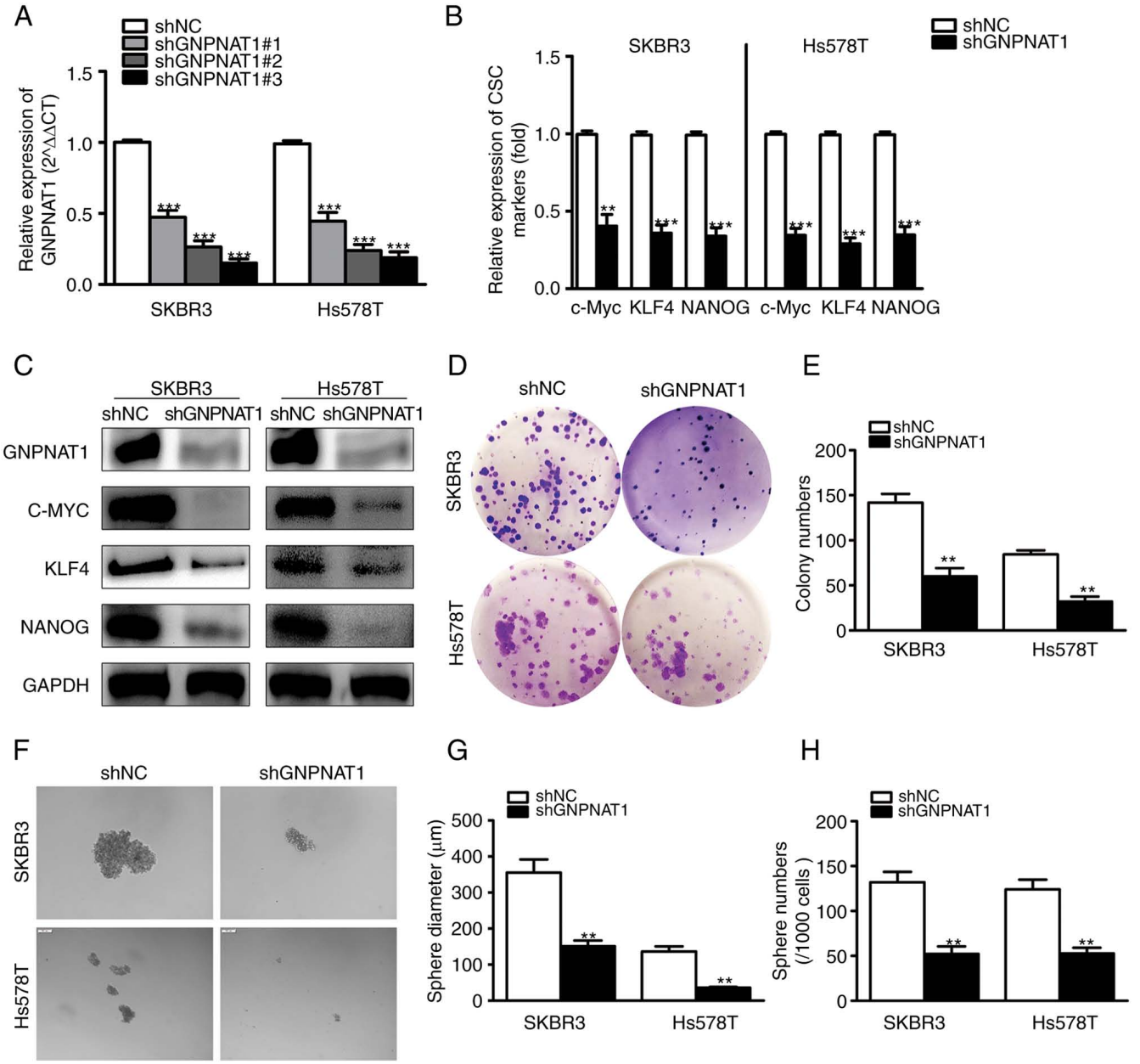

Figure 9. GNPNAT1 knockdown reduces the stemness of BCSCs. (A) Quantitative reverse transcription polymerase chain reaction analysis of the GNPNAT1 knockdown efficiency. Following GNPNAT1 knockdown, (B) mRNA and (C) protein levels of GNPNAT1 in SKBR3 and Hs578T cells decreased. (D) A cell colony formation assay was used to determine the development of BC cells after GNPNAT1 knockdown. (E) The number of G colonies was tallied. (F) Images of mammospheres produced by shGNPNAT1 and shNC cells. The (G) dimension and (H) number of mammospheres in (F) were determined. **P<0.01 and ***P<0.001, as compared with the shNC group. GNPNAT1, glucosamine-phosphate N-acetyltransferase 1; NC, normal control.

and protein (Fig. 10C) expression results of stemness-related genes demonstrated that overexpression of GNPNAT1 caused a significant increase in the expression of c-MYC, KLF4 and NANOG, as compared with the control cells, and GNPNAT1 protein expression was also markedly increased. Similarly, the clonogenic capacity of SKBR3 and Hs578T cells was significantly increased, following GNPNAT1 overexpression (Fig. 10D and E). Finally, the results of spheroid culture experiments demonstrated that GNPNAT1 overexpression caused a significant upregulation of the number and size of suspended spheroids (Fig. 10F-H). The aforementoined results suggested that GNPNAT1 overexpression promoted the stemness of BC cells.

Discussion

Previous research has examined the expression and function of GNPNAT1 in lung cancer (16). GNPNAT1 is an important enzyme, involved in eukaryotic UDP-GlcNAc production and metabolism (35). By interfering with cellular metabolism, GNPNAT1 upregulation may influence the onset and progression of LUAD (36). Nevertheless, the potential predictive usefulness of GNPNAT1 and its expression in BC has not yet been completely investigated. Hence, the aim of the present study was to evaluate the possible function of GNPNAT1 in BC. GNPNAT1 mRNA and protein expression were upregulated in BC tissues, as

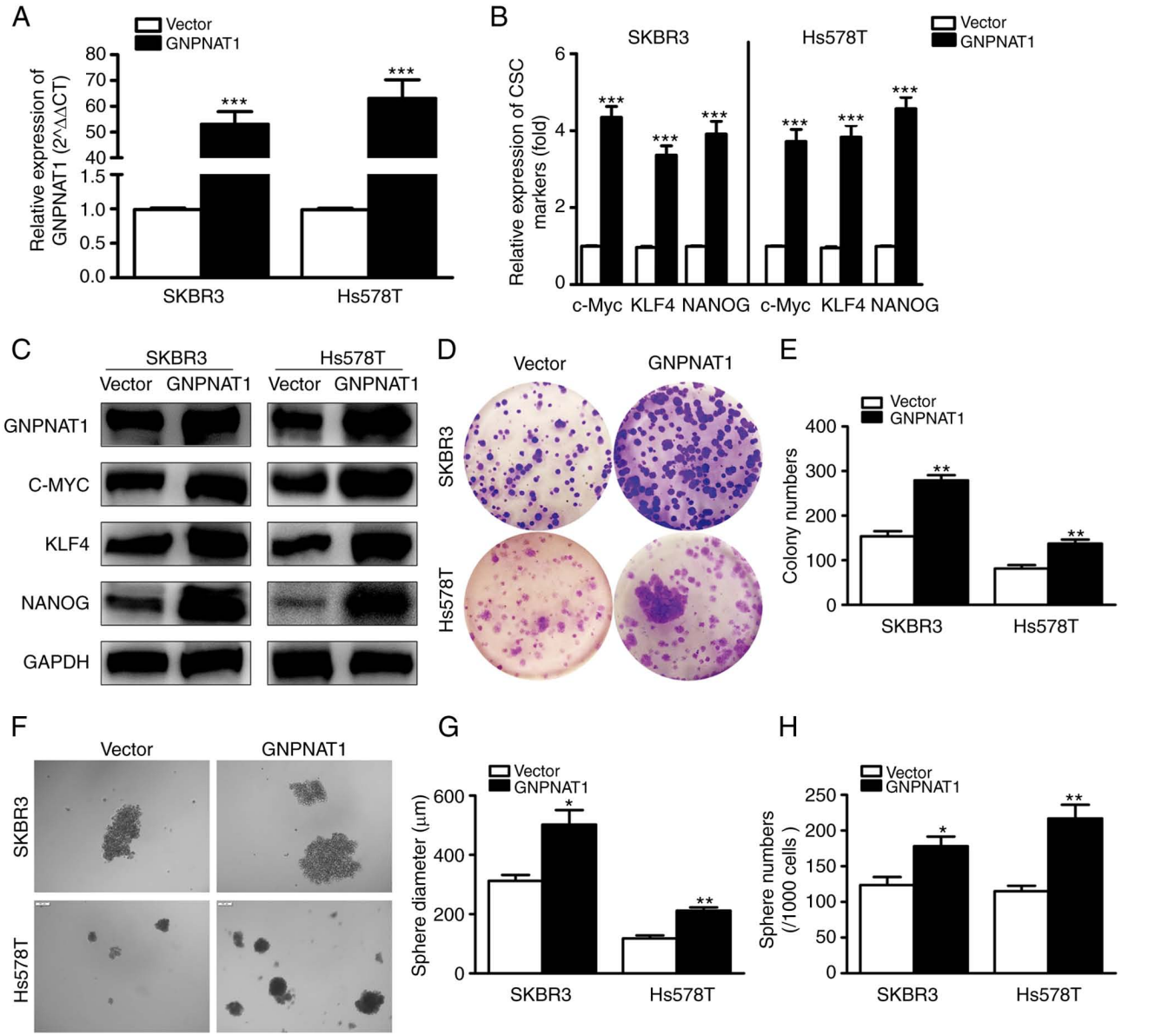

Figure 10. GNPNAT1 overexpression promotes the stemness of BCSCs. (A) GNPNAT1 overexpression efficiency assay, as determined using reverse transcription-quantitative PCR. (B and C) The mRNA and protein expression level of GNPNAT1 in SKBR3 and Hs578T CSCs following GNPNAT1 overexpression. (D and E) Detection of BC cell growth after GNPNAT1 overexpression via cell colony formation assay. (F) Representative images of mammospheres. The (G) diameter and (H) number of mammospheres from F was counted. *P<0.05, **P<0.01 and ***P<0.001, as compared with the vector group. GNPNAT1, glucosamine-phosphate N-acetyltransferase 1; BCSCs, breast cancer stem cells; CSCs, cancer stem cells; BC, breast cancer.

was the expression of GNPNAT1 in several tumor types. ROC curve analysis suggested that GNPNAT1 may be a promising diagnostic biomarker for distinguishing BC from normal tissue. Using Kaplan-Meier curves and univariate analysis, it was demonstrated in the present study that GNPNAT1 expression may be simultaneously linked to both short OS and DSS. GNPNAT1 may function as a biomarker for BC with a poor outcome. In addition, the nomogram revealed that GNPNAT1 may be involved in clinical diagnosis and prognostic evaluation. Further bioinformatics analyses revealed an association between the elevated expression of GNPNAT1 in BC and clinicopathological characteristics (age, TNM pathologic stage, PAM50 and ER/PR/HER2 status). GSEA analysis was performed to further evaluate and identify the influence of GNPNAT1 expression in BC. 'Arachidonic acid metabolism', 'Mucin type O-glycan biosynthesis', 'Carbohydrate digestion and absorption', 'Autophagy', 'Olfactory transduction', and 'alpha-Linolenic acid metabolism' were overrepresented in the GNPNAT1 high expression phenotype. GNPNAT1 may inhibit these processes by modifying the function of cyclin genes post-translationally. *O*-linked N-acetylglucosamine transferase (OGT) is essential for the cell cycle, since inhibiting OGT prevents the synthesis of cyclin D1 (37).

Numerous immune cell types inside the tumor microenvironment (TME) play an essential role in tumor formation, metastasis, and treatment resistance (38). The link between GNPNAT1 expression and immune cell infiltration was then confirmed. Hence, it was hypothesized that GNPNAT1 would promote tumor development and metastasis by

altering the proportion of certain immune cell types that impact the TME. In fact, it has been revealed that GNPNAT1 maintains the TME in LUAD (14,17). The present study revealed a substantial positive link between Th2/T helper cells and GNPNAT1 and a significant negative association between pDC, CD8 T-cells and cytotoxic cells with GNPNAT1. T-cells are an essential component of the TME and tumor-associated $CD4^+$/$CD8^+$ T-cells play a crucial role in the pathophysiology of cancer. Other immune cell types, including interstitial DCs, neutrophils, NK $CD56^+$ bright cells, Th1 cells, DCs and B cells, may potentially affect the survival of tumor cells in the TME. Future research is required, in order to investigate further their connection to GNPNAT1 expression.

Overall, the findings of the present study demonstrate that GNPNAT1 expression may be a viable diagnostic and prognostic molecular marker for patients with BC with a dismal prognosis for survival. Furthermore, arachidonic acid metabolism, mucin-type *O*-glycan production, and other pathways may be controlled by GNPNAT1 in BC. Therefore, further validation trials are necessary to confirm the biological effects of GNPNAT1.

Acknowledgements

Not applicable.

Funding

The present study was supported by the National Natural Science Foundation of China (grant nos. 31501149, 31770815 and 31570764), the Wuhan Health and Family Planning Scientific Research Project (grant no. WX21Q49), the Hubei Natural Science Foundation (grant nos. 2017CFB537, 2019CFB398, 2019CFB368 and 2021CFB230), the Educational Commission of Hubei (grant no. B2020001), the Hubei Province Health and Family Planning Scientific Research Project (grant nos. WJ2021Q051, WJ2019M255 and ZY2021Q005), the Frontier Project of Applied Basic Research in Wuhan (grant no. 2020020601012250) and the Hunan Provincial Natural Science Foundation (grant no. 2023JJ50296) and 'The 14th Five Year Plan' Hubei Provincial advantaged characteristic disciplines (group) project of Wuhan University of Science and Technology (grant no. 2023C0303).

Availability of data and materials

The datasets used and/or analyzed during the current study are available from the corresponding author on reasonable request.

Authors' contributions

XHL, ZYY and TCZ participated in the design of the study. HH, ZWW, SH, YX, YD and FJW performed the experiments and analyzed the data, and HH was mainly responsible for writing this manuscript. HH and ZWW confirm the authenticity of all the raw data. All authors have read and approved the final manuscript.

Ethics approval and consent to participate

Not applicable.

Patient consent for publication

Not applicable.

Competing interests

The authors declare that they have no competing interests.

References

1. Sung H, Ferlay J, Siegel RL, Laversanne M, Soerjomataram I, Jemal A and Bray F: Global Cancer Statistics 2020: GLOBOCAN estimates of incidence and mortality worldwide for 36 cancers in 185 countries. CA Cancer J Clin 71: 209-249, 2021.
2. Zhu J, Wu G, Zhao Y, Yang B, Chen Q, Jiang J, Meng Y, Ji S and Gu K: Epidemiology, treatment and prognosis analysis of small cell breast carcinoma: A population-based study. Front Endocrinol (Lausanne) 13: 802339, 2022.
3. Harbeck N and Gnant M: Breast cancer. Lancet 389: 1134-1150, 2017.
4. Duffy MJ, Walsh S, McDermott EW, and Crown J: Biomarkers in breast cancer: Where are we and where are we going? Adv Clin Chem 71: 1-23, 2015.
5. Bao Z, Cheng J, Zhu J, Ji S, Gu K, Zhao Y, Yu S and Meng Y: Using weighted gene co-expression network analysis to identify increased MND1 expression as a predictor of poor breast cancer survival. Int J Gen Med 15: 4959-4974, 2022.
6. Deng M, Xiong C, He ZK, Bin Q, Song JZ, Li W and Qin J: MCTS1 as a novel prognostic biomarker and its correlation with immune infiltrates in breast cancer. Front Genet 13: 825901, 2022.
7. Rajarajan D, Kaur B, Penta D, Natesh J and Meeran SM: miR-145-5p as a predictive biomarker for breast cancer stemness by computational clinical investigation. Comput Biol Med 135: 104601, 2021.
8. Elhossini RM, Ahmed HA, Otaify G, Ghorab RM, Amr K and Aglan M: A novel variant in GNPNAT1 gene causing a spondylo-epi-metaphyseal dysplasia resembling PGM3-Desbuquois like dysplasia. Am J Med Genet A 188: 2861-2868, 2022.
9. Sabbagh Q, Alkar F, Patte K, Prodhomme O, Janel C, Touraine R, Jeandel C and Geneviève D: A second individual with rhizomelic spondyloepimetaphyseal dysplasia and homozygous variant in GNPNAT1. Eur J Med Genet 65: 104495, 2022.
10. Ain NU, Baroncelli M, Costantini A, Ishaq T, Taylan F, Nilsson O, Mäkitie O and Naz S: Novel form of rhizomelic skeletal dysplasia associated with a homozygous variant in GNPNAT1. J Med Genet 58: 351-356, 2021.
11. Kaushik AK, Shojaie A, Panzitt K, Sonavane R, Venghatakrishnan H, Manikkam M, Zaslavsky A, Putluri V, Vasu VT, Zhang Y, *et al*: Inhibition of the hexosamine biosynthetic pathway promotes castration-resistant prostate cancer. Nat Commun 7: 11612, 2016.
12. Bacos K, Gillberg L, Volkov P, Olsson AH, Hansen T, Pedersen O, Gjesing AP, Eiberg H, Tuomi T, Almgren P, *et al*: Blood-based biomarkers of age-associated epigenetic changes in human islets associate with insulin secretion and diabetes. Nat Commun 7: 11089, 2016.
13. Zhao M, Li H, Ma Y, Gong H, Yang S, Fang Q and Hu Z: Nanoparticle abraxane possesses impaired proliferation in A549 cells due to the underexpression of glucosamine 6-phosphate N-acetyltransferase 1 (GNPNAT1/GNA1). Int J Nanomedicine 12: 1685-1697, 2017.
14. Zheng X, Li Y, Ma C, Zhang J, Zhang Y, Fu Z and Luo H: Independent prognostic potential of GNPNAT1 in lung adenocarcinoma. Biomed Res Int 2020: 8851437, 2020.
15. Zhang S, Zhang H, Li H, Guo J, Wang J and Zhang L: Potential role of glucosamine-phosphate N-acetyltransferase 1 in the development of lung adenocarcinoma. Aging (Albany NY) 13: 7430-7453, 2021.

16. Zhu P, Gu S, Huang H, Zhong C, Liu Z, Zhang X, Wang W, Xie S, Wu K, Lu T and Zhou Y: Upregulation of glucosamine-phosphate N-acetyltransferase 1 is a promising diagnostic and predictive indicator for poor survival in patients with lung adenocarcinoma. Oncol Lett 21: 488, 2021.
17. Liu W, Jiang K, Wang J, Mei T, Zhao M and Huang D: Upregulation of GNPNAT1 predicts poor prognosis and correlates with immune infiltration in lung adenocarcinoma. Front Mol Biosci 8: 605754, 2021.
18. Gupta PB, Fillmore CM, Jiang G, Shapira SD, Tao K, Kuperwasser C and Lander ES: Stochastic state transitions give rise to phenotypic equilibrium in populations of cancer cells. Cell 146: 633-644, 2011.
19. Kreso A and Dick JE: Evolution of the cancer stem cell model. Cell Stem Cell 14: 275-291, 2014.
20. Al-Hajj M, Wicha MS, Benito-Hernandez A, Morrison SJ and Clarke MF: Prospective identification of tumorigenic breast cancer cells. Proc Natl Acad Sci USA 100: 3983-3988, 2003.
21. Charafe-Jauffret E, Ginestier C, Bertucci F, Cabaud O, Wicinski J, Finetti P, Josselin E, Adelaide J, Nguyen TT, Monville F, *et al*: ALDH1-positive cancer stem cells predict engraftment of primary breast tumors and are governed by a common stem cell program. Cancer Res 73: 7290-7300, 2013.
22. Chandrashekar DS, Karthikeyan SK, Korla PK, Patel H, Shovon AR, Athar M, Netto GJ, Qin ZS, Kumar S, Manne U, *et al*: UALCAN: An update to the integrated cancer data analysis platform. Neoplasia 25: 18-27, 2022.
23. Chandrashekar DS, Bashel B, Balasubramanya SAH, Creighton CJ, Ponce-Rodriguez I, Chakravarthi BVSK and Varambally S: UALCAN: A portal for facilitating tumor subgroup gene expression and survival analyses. Neoplasia 19: 649-658, 2017.
24. Zhang Y, Chen F, Chandrashekar DS, Varambally S and Creighton CJ: Proteogenomic characterization of 2002 human cancers reveals pan-cancer molecular subtypes and associated pathways. Nat Commun 13: 2669, 2022.
25. Chen F, Chandrashekar DS, Varambally S and Creighton CJ: Pan-cancer molecular subtypes revealed by mass-spectrometry-based proteomic characterization of more than 500 human cancers. Nat Commun 10: 5679, 2019.
26. Uhlén M, Fagerberg L, Hallström BM, Lindskog C, Oksvold P, Mardinoglu A, Sivertsson Å, Kampf C, Sjöstedt E, Asplund A, *et al*: Proteomics. Tissue-based map of the human proteome. Science 347: 1260419, 2015.
27. Vasaikar SV, Straub P, Wang J and Zhang B: LinkedOmics: Analyzing multi-omics data within and across 32 cancer types. Nucleic Acids Res 46(D1): D956-D963, 2018.
28. Wang J, Vasaikar S, Shi Z, Greer M and Zhang B: WebGestalt 2017: A more comprehensive, powerful, flexible and interactive gene set enrichment analysis toolkit. Nucleic Acids Res 45(W1): W130-W137, 2017.
29. Ru B, Wong CN, Tong Y, Zhong JY, Zhong SSW, Wu WC, Chu KC, Wong CY, Lau CY, Chen I, *et al*: TISIDB: An integrated repository portal for tumor-immune system interactions. Bioinformatics 35: 4200-4202, 2019.
30. Park SY: Nomogram: An analogue tool to deliver digital knowledge. J Thorac Cardiovasc Surg 155: 1793, 2018.
31. Hu H, Xiang Y, Zhang XY, Deng Y, Wan FJ, Huang Y, Liao XH and Zhang TC: CDCA5 promotes the progression of breast cancer and serves as a potential prognostic biomarker. Oncol Rep 48: 172, 2022.
32. Livak KJ and Schmittgen TD: Analysis of relative gene expression data using real-time quantitative PCR and the 2(-Delta Delta C(T)) Method. Methods 25: 402-408, 2001.
33. Ai L, Mu S, Sun C, Fan F, Yan H, Qin Y, Cui G, Wang Y, Guo T, Mei H, *et al*: Myeloid-derived suppressor cells endow stem-like qualities to multiple myeloma cells by inducing piRNA-823 expression and DNMT3B activation. Mol Cancer 18: 88, 2019.
34. Ma XL, Hu B, Tang WG, Xie SH, Ren N, Guo L and Lu RQ: CD73 sustained cancer-stem-cell traits by promoting SOX9 expression and stability in hepatocellular carcinoma. J Hematol Oncol 13: 11, 2020.
35. Aquino-Gil M, Pierce A, Perez-Cervera Y, Zenteno E and Lefebvre T: OGT: A short overview of an enzyme standing out from usual glycosyltransferases. Biochem Soc Trans 45: 365-370, 2017.
36. Furuta E, Okuda H, Kobayashi A and Watabe K: Metabolic genes in cancer: Their roles in tumor progression and clinical implications. Biochim Biophys Acta 1805: 141-152, 2010.
37. Olivier-Van Stichelen S, Drougat L, Dehennaut V, El Yazidi-Belkoura I, Guinez C, Mir AM, Michalski JC, Vercoutter-Edouart AS and Lefebvre T: Serum-stimulated cell cycle entry promotes ncOGT synthesis required for cyclin D expression. Oncogenesis 1: e36, 2012.
38. Usui T, Sakurai M, Enjoji S, Kawasaki H, Umata K, Ohama T, Fujiwara N, Yabe R, Tsuji S, Yamawaki H, *et al*: Establishment of a novel model for anticancer drug resistance in three-dimensional primary culture of tumor microenvironment. Stem Cells Int 2016: 7053872, 2016.